JOURNAL OF THEORETICAL
AND APPLIED MECHANICS
40, 4, pp. 847-871, Warsaw 2002

ON ORIGIN OF UNSTABLE MODES IN VISCOUS CHANNEL FLOW SUBJECT TO PERIODICALLY DISTRIBUTED SURFACE SUCTION

JACEK SZUMBARSKI

Institute of Aeronautics and Applied Mechanics, Warsaw University of Technology
e-mail: jasz@meil.pw.edu.pl

The linear stability of a flow in a channel subject to periodically distributed suction applied at the walls is investigated. The focus is on the relation between unstable modes observed in such a flow and the stability properties of the flow without suction (the Poiseuille flow). It is demonstrated that linearly unstable modes appearing in the presence of suction can be interpreted as modified Orr-Sommerfeld's or Squire's eigenmodes of the Poiseuille flow. Originally, these modes have the streamwise wave number equal to zero, i.e. they are invariant in the streamwise direction. When the surface suction is applied, the modes are additionally modulated along the channel and they become dependent on the streamwise variable. In the range of the parameters studied, a pair of such modes, one Orr-Sommerfeld's and one Squire's, can be simultaneously unstable. Certain properties of these modes are discussed in some details. Specifically, the influence of non-symmetric suction on stability characteristics is analysed.

Key words: periodic channel flow, linear stability, Floquet theory, surface suction

1. Introduction

Floryan (1997) investigated the linear stability of flows in a channel with periodically distributed surface suction. The admissible form of perturbations of the steady state were defined within the framework of the Floquet theory. Recently, using similar approach, Cabal et al. (2002) analysed the stability of a flow in a channel with periodically corrugated walls. The important conclusion from both studies is that the introduction of a space-periodic modification of the boundary data, either geometric or through surface suction, reduces signi-

ficantly the critical Reynolds number. The most amplified disturbances correspond to purely imaginary eigenvalues and have a form of three-dimensional streamwise vortices. In the plain Poiseuille flow, the critical disturbances have a form of two-dimensional travelling waves (TS waves), while all eigenmodes with purely imaginary eigenvalues are damped.

In this work, the channel flow modified by periodically distributed surface suction is revisited. The objective is to shed light on the following issues:

a) is the eigensolution described in Floryan (1997) the only possible form of instability predicted by the linear theory,

b) what kind of relation exists between the eigensolutions obtained in the linear stability analysis of the original Poiseuille flow and the flow modified by distributed surface suction?

The paper is organized as follows. Governing equations for the main flow and the equations of the linear stability are presented in Section 2. Numerical techniques of determination of the main flow and its stability characteristics are described briefly in Section 3. Results of numerical computations are discussed in Section 4. It is shown that in certain parameter range another unstable mode can co-exist along with the mode described in Floryan (1997). Then, the problem of the origin of both unstable modes is addressed. Using the method of inverse iterations as a tool for "tracing" selected eigenvalues in the parameter space, we explain the relation between the relevant parts of the spectra for the Poiseuille flow and the flow modified by the suction. It is demonstrated that the unstable modes originate from certain universal (independent on the velocity distribution) class of eigensolutions of the linear stability problem formulated for a general parallel flow. The properties of these eigensolutions are described in some details. Finally, the crucial role of the symmetry between the suction distribution at the channel walls is discussed.

2. Problem formulation

2.1. Reference flow

Consider a plane Poiseuille flow confined between flat rigid walls at $y = \pm 1$ and extending to infinity in the x-direction. The corresponding velocity and pressure fields are following

$$\begin{aligned} \boldsymbol{V}_0(\boldsymbol{x}) &= [u_0(x,y), v_0(x,y)] = [u_0(y), 0] = [1-y^2, 0] \\ p_0(\boldsymbol{x}) &= -\frac{2x}{\mathrm{Re}} \end{aligned} \tag{2.1}$$

where the fluid is directed towards the positive x-axis and the Reynolds number Re is based on the half-channel height and the maximum x-velocity. This flow is driven by a constant negative pressure gradient.

2.2. Flow in the channel with distributed suction

Assume that the reference flow is modified by suction applied at both channel walls. The suction velocity is oriented perpendicularly to the walls. The distributions of the wall-normal velocity component at the walls are defined as $v_L(x)$ and $v_U(x)$ for the lower and upper wall, respectively. These distributions are assumed periodic with the wavelength $\lambda_x = 2\pi/\alpha$. The functions $v_L(x)$ and $v_U(x)$ can be expressed in terms of a Fourier series in the form

$$v_L(x) = \sum_{n=-\infty}^{n=\infty} (V_n)_L \mathrm{e}^{\mathrm{i}n\alpha x} \qquad v_U(x) = \sum_{n=-\infty}^{n=\infty} (V_n)_U \mathrm{e}^{\mathrm{i}n\alpha x} \tag{2.2}$$

where $(V_n)_L = (V_{-n})_L^*$ and $(V_n)_L = (V_{-n})_L^*$ in order for $v_U(x)$ and $v_L(x)$ to be real. Additionally, it is assumed that $(V_0)_L = (V_0)_U = 0$ i.e., the volume flux due to the suction per one geometrical period is zero.

The flow in the channel can be represented as

$$\begin{aligned} \boldsymbol{V}(\boldsymbol{x}) &= [u(x,y), v(x,y)] = \boldsymbol{V}_0(\boldsymbol{x}) + \boldsymbol{V}_1(\boldsymbol{x}) = [u_0(y), 0] + [u_1(x,y), v_1(x,y)] \\ p(\boldsymbol{x}) &= p_0(\boldsymbol{x}) + p_1(\boldsymbol{x}) \end{aligned} \tag{2.3}$$

where $\boldsymbol{V}_1$ and p_1 are the velocity and pressure modifications of reference flow (2.1) caused by the wall suction. Substitution of the above representations of the flow quantities into the Navier-Stokes and continuity equations results in the following form of the governing equations

$$\begin{aligned} u_0\partial_x u_1 + u_1\partial_x u_1 + v_1 D u_0 + v_1\partial_y u_1 &= -\partial_x p_1 + \frac{1}{\mathrm{Re}}(\partial_{xx}u_1 + \partial_{yy}u_1) \\ u_0\partial_x v_1 + u_1\partial_x v_1 + v_1\partial_y v_1 &= -\partial_y p_1 + \frac{1}{\mathrm{Re}}(\partial_{xx}v_1 + \partial_{yy}v_1) \\ \partial_x u_1 + \partial_y v_1 &= 0 \end{aligned} \tag{2.4}$$

where the symbols ∂ denotes partial differentiation, the subscripts x and y denote the arguments of partial differentiation, and $D = d/dy$. Introduction of the streamfunction defined as

$$u_1 = \partial_y \Psi \qquad v_1 = -\partial_x \Psi$$

and elimination of the pressure entails an expression of field equations (2.4) in the form

$$(u_0\partial_x + \partial_y\Psi\partial_x - \partial_x\Psi\partial_y)\Delta\Psi - D^2u_0\partial_x\Psi = \frac{1}{\mathrm{Re}}\Delta^2\Psi \tag{2.5}$$

where Δ denotes the Laplace operator. Since u_1 and v_1 are periodic in x with the period $\lambda_x = 2\pi/\alpha$, the streamfunction can be represented as

$$\Psi(x,y) = \sum_{n=-\infty}^{+\infty} \Phi_n(y)\mathrm{e}^{\mathrm{i}n\alpha x} \tag{2.6}$$

where $\Phi_n = \Phi^*_{-n}$ in order for Ψ_n to be real.

The following nonlinear system of ordinary differential equations can be derived for the amplitude functions Φ_n, $n = -1, 0, 1, ...$

$$\begin{aligned}&[D_n^2 - \mathrm{i}n\alpha\mathrm{Re}(u_0D_n - D^2u_0)]\Phi_n - \\ &-\mathrm{i}\alpha\mathrm{Re}\sum_{k=-\infty}^{+\infty}[kD\Phi_{n-k}D_k\Phi_k - (n-k)\Phi_{n-k}D_kD\Phi_k] = 0\end{aligned} \tag{2.7}$$

where $D_n = D^2 - n^2\alpha^2$. Equation (2.7) has been obtained by substituting (2.6) into (2.5) and separating the Fourier components. In particular, the equation for the amplitude function Φ_0 can be written as follows

$$D^4\Phi_0 + 2\alpha\mathrm{Re}\cdot\mathrm{Im}\Big\{\sum_{k=1}^{\infty} k[(D\Phi_k)^*D^2\Phi_k + (\Phi_k)^*D^3\Phi_k]\Big\} = 0 \tag{2.8}$$

The boundary conditions are imposed on the velocity modification components

$$\left.\begin{aligned}u_1(x,-1) &= 0\\ v_1(x,-1) &= v_L(x)\end{aligned}\right\} \quad \text{at the bottom wall}$$
$$\left.\begin{aligned}u_1(x,1) &= 0\\ v_1(x,1) &= v_U(x)\end{aligned}\right\} \quad \text{at the upper wall} \tag{2.9}$$

With the use of the Fourier expansions, conditions (2.9) yield

$$\begin{aligned} &\Phi_n(-1) = \frac{\mathrm{i}(V_n)_L}{n\alpha} && \Phi_n(1) = \frac{\mathrm{i}(V_n)_U}{n\alpha} \\ &D\Phi_n(-1) = D\Phi_n(1) = 0 && |n| > 0 \end{aligned} \tag{2.10}$$

The boundary conditions for the amplitude function Φ_0 can be defined in many ways. Here, it is assumed that that resulting flow is characterised by the mean volume flux equal to the volume flux of the reference Poiseuille flow. This assumption yields

$$\Phi_0(-1) = \Phi_0(1) \qquad D\Phi_0(-1) = D\Phi_0(1) \tag{2.11}$$

The other possible choice of the boundary conditions for Φ_0 is to prescribe the value of the mean pressure gradient. The reader is advised to refer to Floryan (1997) for further details.

2.3. Linear stability problem

Assume that the nonlinear boundary problems defined by differential equations (2.8), (2.9) and boundary conditions (2.10), (2.11) have been solved. Then, the modification part of the resulting velocity field is given by

$$\begin{aligned} u_1(x,y) &\equiv \sum_{k=-\infty}^{+\infty} f_u^k(y)\exp(\mathrm{i}k\alpha x) = \sum_{k=-\infty}^{+\infty} D\psi_k(y)\exp(\mathrm{i}k\alpha x) \\ v_1(x,y) &\equiv \sum_{k=-\infty}^{+\infty} f_v^k(y)\exp(\mathrm{i}k\alpha x) = \sum_{k=-\infty}^{+\infty} \mathrm{i}k\alpha\psi_k(y)\exp(\mathrm{i}k\alpha x) \end{aligned} \tag{2.12}$$

The complete velocity field of the main flow is a sum of the reference flow and the modification

$$\boldsymbol{V}_1(x,y) = [u_0(y),0,0] + \sum_{k=-\infty}^{+\infty} [f_u^k(y), f_v^k(y), 0]\exp(\mathrm{i}k\alpha x) \tag{2.13}$$

In order to analyse the stability properties of the obtained flow, see (2.13), a perturbed velocity field is introduced

$$\boldsymbol{V} = \boldsymbol{V}_1(x,y) + \boldsymbol{V}_2(t,x,y,z) \tag{2.14}$$

The velocity field of the main flow $\boldsymbol{V}_1$ is x-periodic, and thus the admissible form of the disturbance velocity field $\boldsymbol{V}_2$ is defined within the framework of the Floquet theory as

$$\boldsymbol{V}_2(t,x,y,z) = \sum_{m=-\infty}^{+\infty} [g_u^m(y), g_v^m(y), g_w^m(y)] \exp[\mathrm{i}(t_m x + \beta z - \lambda t)] \tag{2.15}$$

In the above expression $t_m = \delta + m\alpha$, β denotes the spanwise wave number of the disturbance and δ denotes the Floquet exponent. The reader may notice that, in general, the disturbance field can be quasi-periodic in the x variable.

The next step is to derive equations governing the evolution of the disturbance velocity field $\boldsymbol{V}_2(t,x,y,z)$. Afterwards, the insertion of representation (2.15) into these equations will yield homogeneous boundary problems for the amplitudes $\{g_u^m(y), g_v^m(y), g_w^m(y),\ m = ..., -1, 0, 1, ...\}$.

Following the derivation presented in Floryan (1997), we begin with the velocity-vorticity formulation of the governing equations for full, disturbed velocity field (2.14)

$$\begin{aligned} &\frac{\partial \boldsymbol{\omega}}{\partial t} + (\boldsymbol{V}\nabla)\boldsymbol{\omega} - (\boldsymbol{\omega}\nabla)\boldsymbol{V} = \frac{1}{\mathrm{Re}}\nabla^2\boldsymbol{\omega} \\ &\nabla\cdot\boldsymbol{V} = 0 \qquad\qquad \boldsymbol{\omega} = \nabla\times\boldsymbol{V} \end{aligned} \tag{2.16}$$

The disturbed velocity field is a sum of the main flow and the disturbance defined by (2.15). Consequently, the vorticity field can be expressed as follows

$$\boldsymbol{\omega} = \boldsymbol{\omega}_1(x,y) + \boldsymbol{\omega}_2(t,x,y,z) \tag{2.17}$$

Insertion of (2.14) and (2.17) into equations (2.16), and dropping nonlinear terms yield

$$\begin{aligned} &\frac{\partial \boldsymbol{\omega}_2}{\partial t} + (\boldsymbol{V}_1\nabla)\boldsymbol{\omega}_2 - (\boldsymbol{\omega}_2\nabla)\boldsymbol{V}_1 + (\boldsymbol{V}_2\nabla)\boldsymbol{\omega}_1 - (\boldsymbol{\omega}_1\nabla)\boldsymbol{V}_2 = \frac{1}{\mathrm{Re}}\nabla^2\boldsymbol{\omega}_2 \\ &\nabla\cdot\boldsymbol{V}_2 = 0 \qquad\qquad \boldsymbol{\omega}_2 = \nabla\times\boldsymbol{V}_2 \end{aligned} \tag{2.18}$$

It is convenient to formulate the stability problem in terms of a different set of unknowns. Consider the wall-normal component of the disturbance vorticity field

$$\omega_{2y} = \frac{\partial v_{2x}}{\partial z} - \frac{\partial v_{2z}}{\partial x} \tag{2.19}$$

which can be expressed as follows

$$\omega_{2y}(t,x,y,z) = -\mathrm{i}\sum_{m=-\infty}^{+\infty} \theta^m(y) \exp[\mathrm{i}(t_m x + \beta z - \lambda t)] \tag{2.20}$$

The new set of the amplitude functions $\{\theta^m,\ m = ..., -1, 0, 1, ...\}$ is related to the formerly defined one as

$$\theta^m = -\beta g_u^m + t_m g_w^m \tag{2.21}$$

The inverse relations can be found with the use of the Fourier form of the continuity equation

$$\mathrm{i}t_m g_u^m + D g_v^m + \mathrm{i}\beta g_w^m = 0 \qquad m = ..., -2, -1, 0, 1, 2, ... \tag{2.22}$$

in the following form

$$g_u^m = \frac{1}{k_m^2}(\mathrm{i}t_m D g_v^m - \beta\theta^m) \qquad g_w^m = \frac{1}{k_m^2}(\mathrm{i}\beta D g_v^m + t_m\theta^m) \tag{2.23}$$

where $k_m^2 = t_m^2 + \beta^2$.

After rather lengthy algebra, the following (infinite) set of linear ODEs can be derived $(m = ..., -1, 0, 1, ...)$

$$S^{(m)} g_v^m + \mathrm{Re}\sum_{n=1}^{\infty}(\overline{G}_v^{(m,n)} g_v^{m+n} + G_v^{(m,n)} g_v^{m-n} + \overline{G}_\theta^{(m,n)}\theta^{m+n} + G_\theta^{(m,n)}\theta^{m-n}) = 0 \tag{2.24}$$

$$T^{(m)}\theta^m + \mathrm{Re}\beta D F_u^0 g_v^m +$$
$$+\mathrm{Re}\sum_{n=1}^{\infty}(\overline{E}_v^{(m,n)} g_v^{m+n} + E_v^{(m,n)} g_v^{m-n} + \overline{E}_\theta^{(m,n)}\theta^{m+n} + E_\theta^{(m,n)}\theta^{m-n}) = 0$$

where the operators are defined in the following way

$$\begin{aligned}
S^{(m)} &= (D^2 - k_m^2)^2 - \mathrm{iRe}[(t_m F_u^0 - \lambda)(D^2 - k_m^2) - t_m D^2 F_u^0] \\
G_v^{(m,n)} &= \frac{\mathrm{i}n\alpha}{k_{m-n}^2}(\beta^2 - t_m t_{m-n}) D f_u^n D + \frac{k_m^2}{k_{m-n}^2}(\beta^2 + t_{m-n}t_{m-2n}) f_v^n D + \\
&+ \frac{\mathrm{i}}{k_{m-n}^2}(2n\alpha\beta^2 - t_m k_{m-n}^2) f_u^n D^2 + \frac{\mathrm{i}}{k_{m-n}^2}(n\alpha t_m - k_m^2) f_v^n D^3 + \\
&+ \mathrm{i}k_m^2 t_{m-2n} f_u^n + \mathrm{i}t_m D^2 f_u^n \\
\overline{G}_v^{(m,n)} &= \frac{\mathrm{i}n\alpha}{k_{m+n}^2}(t_m t_{m+n} - \beta^2)(D f_u^n)^* D + \frac{k_m^2}{k_{m+n}^2}(\beta^2 + t_{m+n}t_{m+2n})(f_v^n)^* D + \\
&+ \frac{\mathrm{i}}{k_{m+n}^2}(-2n\alpha\beta^2 - t_m k_{m+n}^2)(f_u^n)^* D^2 + \\
&+ \frac{\mathrm{i}}{k_{m+n}^2}(-n\alpha t_m - k_m^2)(f_v^n)^* D^3 + \mathrm{i}k_m^2 t_{m+2n}(f_u^n)^* + \mathrm{i}t_m (D^2 f_u^n)^*
\end{aligned}$$

$$
\begin{aligned}
G_\theta^{(m,n)} &= \frac{1}{k_{m-n}^2} 2n\alpha\beta t_{m-n} f_u^n D + \frac{n\alpha\beta}{k_{m-n}^2}(t_m + t_{m-n}) D f_u^n - \frac{\mathrm{i}n\alpha\beta k_m^2}{k_{m-n}^2} f_u^n - \\
&- \frac{\mathrm{i}n\alpha\beta}{k_{m-n}^2} f_u^n D^2 \\
\overline{G}_\theta^{(m,n)} &= -\frac{1}{k_{m+n}^2} 2n\alpha\beta t_{m+n} (f_u^n)^* D - \frac{n\alpha\beta}{k_{m+n}^2}(t_m + t_{m+n})(D f_u^n)^* + \\
&+ \frac{\mathrm{i}n\alpha\beta k_m^2}{k_{m+n}^2}(f_u^n)^* + \frac{\mathrm{i}n\alpha\beta}{k_{m+n}^2}(f_u^n)^* D^2 \\
T^{(m)} &= D^2 - k_m^2 - \mathrm{iRe}(t_m F_u^0 - \lambda) \\
E_v^{(m,n)} &= \beta D f_u^n - \frac{\mathrm{i}n\alpha\beta}{k_{m-n}^2} f_v^n D^2 \\
\overline{E}_v^{(m,n)} &= \beta (D f_u^n)^* + \frac{\mathrm{i}n\alpha\beta}{k_{m+n}^2}(f_v^n)^* D^2 \\
E_\theta^{(m,n)} &= -\mathrm{i}t_m f_u^m - \frac{1}{k_{m-n}^2}(\beta^2 + t_m t_{m-n}) f_v^n D \\
\overline{E}_\theta^{(m,n)} &= -\mathrm{i}t_m (f_u^m)^* - \frac{1}{k_{m+n}^2}(\beta^2 + t_m t_{m+n})(f_v^n)^* D \\
F_u^0 &= u_0 + f_u^0
\end{aligned}
$$

The homogeneous boundary conditions for the amplitude functions are

$$
g_v^m(\pm 1) = D g_v^m(\pm 1) = 0 \qquad \theta^m(\pm 1) = 0 \qquad m = ..., -1, 0, 1, ... \quad (2.25)
$$

The objective is to solve the eigenvalue/eigenfunction problem for set of linear ODEs (2.24) subject to boundary conditions (2.25). It means that one is interested in the determination of such values of the complex parameter λ (eigenvalues), that the considered boundary problem has nontrivial solutions (eigenfunctions). The imaginary parts of the eigenvalues determine the temporal behavior of the disturbances. If all eigenvalues have negative imaginary parts all disturbances will eventually decay and the flow is (linearly) stable. Otherwise, it exists at least one form of the disturbance that will grow exponentially in time, no matter how small its initial magnitude is. In order to obtain a tractable algebraic eigenvalue problem, discretisation of the differential boundary problem has to be applied. Some details of this procedure are given in the following section.

3. Numerical discretisation method

3.1. The main flow

The problem to be solved numerically consists of the infinite system of nonlinear ordinary differential equations (2.7) with the boundary conditions (2.10). The solution method follows closely the numerical technique proposed in Szumbarski and Floryan (1999) for flows in a channel with corrugated walls. The main difference is in the treatment of the boundary conditions which, in the case of wall suction, is much simpler.

The discretisation procedure consists of several steps:

(a) Truncation of the Fourier representation to a finite number of the modes

$$\Psi(x,y) \approx \sum_{n=-M_F}^{M_F} \Phi_n(y) \mathrm{e}^{\mathrm{i}n\alpha x} \tag{3.1}$$

and choosing a finite subset of the differential equations and the boundary conditions so that a complete boundary value problem is defined.

(b) Approximation of the unknown amplitude functions by the finite Chebyshev expansions

$$\Phi_n(y) = \sum_{j=0}^{+\infty} G_j^n T_j(y) \approx \sum_{j=0}^{J} G_j^n T_j(y) \tag{3.2}$$

and insertion of them into the differential equations. This step involves differentiation of the Chebyshev expansions and computing their products. Both types of operations are performed using exact formulas derived in the theory of the Chebyshev polynomials.

(c) Derivation of the nonlinear algebraic equations for the Chebyshev coefficients $\{G_j^n\}$. This step involves separation of the expressions standing at each Chebyshev polynomial up to the order $J-4$ in all equations.

(d) Completion of the system by adding algebraic equations derived from the boundary conditions. There are four such equations for each amplitude function.

As a result, the system of $J(MF+1)$ nonlinear algebraic equations is obtained. The reader may note that the discretisation described above is simply a tau-Galerkin method based on the Chebyshev polynomials. In order to find

the solution, one can apply any of standard tools, e.g. the Newton iterations. Here, however, a different approach has been taken up. It can be noticed that the coupling between the equations is only via the nonlinear terms. This property is inherited by the corresponding algebraic problem. This means that one can move all nonlinear terms of the right-hand sides and obtain a system with uncoupled left-hand sides. Such a structure suggests a solution method consisting in iterative solving of a sequence of separated linear problems. Each of these problems is of dimension J and the order is, in essence, arbitrary. Here, solving in the reverse order has been implemented, i.e. the subsystem for the amplitude function Φ_M is solved first and eventually the mode zero is upgraded as the last one in each iteration.

It should be clear that, due to the nonlinearity, the flow response is always multi-modal, even if the wall suction has a form of a single Fourier harmonic. Intuitively, the length of the Fourier representation of the approximate solution should be, say, several times longer than the Fourier representation of the multi-modal wall suction. In the case of the suction in the form of a single Fourier harmonic with a sufficiently small amplitude, the linearised model can be applied (see Floryan, 1997). In the current work, the multi-mode (6 modes) is used, although the range of the parameters studied is mostly covered by the linear theory.

3.2. Linear stability equations

Linear differential equations (2.24) are discretised in a similar way as equations (2.7) for the main flow. First, it is assumed that the disturbance velocity and vorticity fields can be approximated by a finite number of modes

$$\boldsymbol{V}_2(t,x,y,z) \approx \sum_{m=-M_S}^{M_S} [g_u^m(y), g_v^m(y), g_w^m(y)] \exp[\mathrm{i}(t_m x + \beta z - \lambda t)]$$
$$\omega_{2y}(t,x,y,z) \approx -\mathrm{i} \sum_{m=-M_S}^{M_S} \theta^m(y) \exp[\mathrm{i}(t_m x + \beta z - \lambda t)] \tag{3.3}$$

The amplitude functions g_v^n and θ^n ($n = -M_S, -M_S+1, ...0, ..., M_S-1, M_S$) are approximated by their Chebyshev expansions. Assume, N_v denotes the order of expansions used to approximate the amplitude functions g_v^n, while N_θ denotes the order of expansions of the amplitude functions θ^n, for $n = -M_S, -M_S+1, ..., 0, ..., M_S-1, M_S$. These expansions are inserted into the stability equations. Some coefficients in these equations are dependent on the y variable as they involve the amplitude functions of the main flow and

their derivatives. They are expressed in terms of the Chebyshev expansions with the previously computed coefficients. Insertion of all Chebyshev expansions into the stability equations and separations of the expressions standing at each polynomial yield a linear algebraic system. More precisely, $N_v - 4$ algebraic equations are derived from each differential equation of the fourth order $(2.24)_1$, and $N_\theta - 2$ algebraic equations are derived from each equation of the second order $(2.24)_2$. Boundary conditions (2.25) give six additional linear equations to each pair of the unknowns g_v^n and θ^n. As a result, we obtain a large set of $(2M_S + 1)(N_v + N_\theta + 2)$ linear algebraic equations, which defines the generalized eigenvalue problem

$$\mathbf{P}\boldsymbol{c} = \lambda \mathbf{Q}\boldsymbol{c} \tag{3.4}$$

The flow is linearly stable when no eigenvalue with the positive imaginary part exists.

Various methods can be used to solve eigenvalue problem (3.4). In the stability analysis, we are usually interested in the localisation of one or perhaps several eigenvalues with the largest imaginary parts, as they correspond to the most "dangerous" forms of disturbances. We are also interested in the variation of these eigenvalues (and possibly the corresponding eigenfunctions) with the parameters like the Reynolds number, the suction magnitude or the wave numbers. Such parameter "tracing" can be carried out effectively by the Inverse Iterations Method (see Saad, 1992).

4. Discussion of results

In this section, results of numerical computations are presented. The distributed surface suction is assumed in the form of a single Fourier mode at each wall of the channel, i.e.

$$V_L(x) = S_L \cos(\alpha x) \qquad V_U(x) = S_U \cos(\alpha x + \phi)$$

All results discussed in this section have been obtained for the Reynolds number Re=5000.

Solving numerically generalized eigenvalue problem (3.4), one can find two unstable modes. The corresponding eigenvalues are purely imaginary. The first (more attenuated) mode is the one described by Floryan (1997). The other mode is unstable in a narrower range of the wave numbers and its amplification rate is lower. For higher streamwise wave numbers, however, both modes are

amplified at nearly the same rate. In Fig. 1, we show the imaginary part of both eigenvalues plotted as functions of the spanwise wave number β, for different suction wave numbers α. Fig. 2 presents the spanwise structure of the disturbance velocity field of the unstable modes, computed for $\alpha = 3$, $\beta = 2$, $\phi = \pi$ and the wall corrugation amplitudes $S = S_L = S_U = 6.0 \cdot 10^{-3}$.

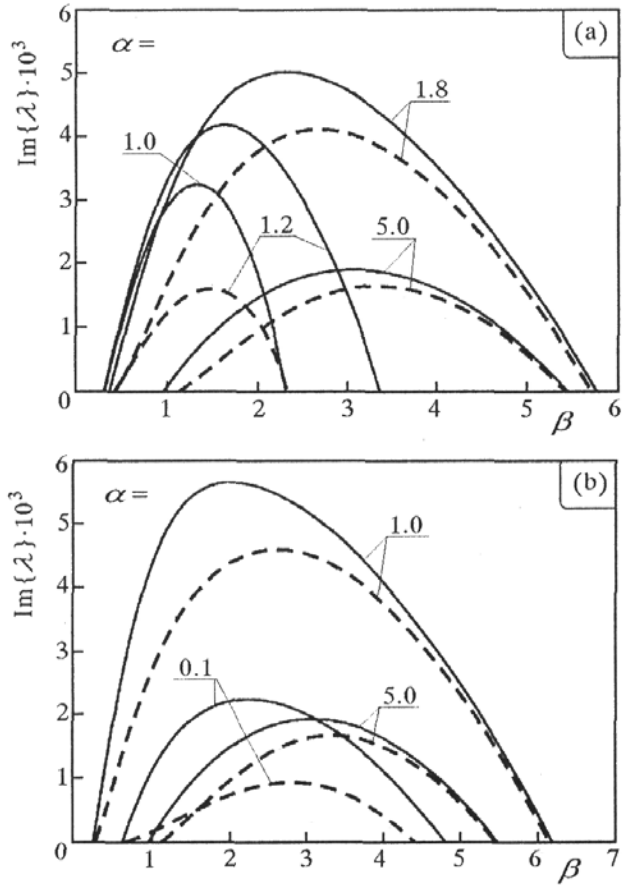

Fig. 1. Amplification rates of the first (solid line) and second (dashed line) unstable modes plotted as functions of the spanwise wave number β, computed for $S = 6 \cdot 10^{-3}$, Re=5000 and (a) symmetric suction ($\phi = 0$), (b) anti-symmetric suction ($\phi = \pi$)

In order to explain the origin of the unstable modes, one should find a relation between the computed eigenvalues and the spectrum of the flow in the channel without suction, i.e. the Poiseuille flow. Such a relation can be established by tracing the variation of the eigenvalues while the suction amplitudes are decreased to zero. One of possible ways of such magnitude reduction is to begin with the same amplitudes at both walls and then to proceed towards zero while keeping them equal. The result of that procedure is presented in

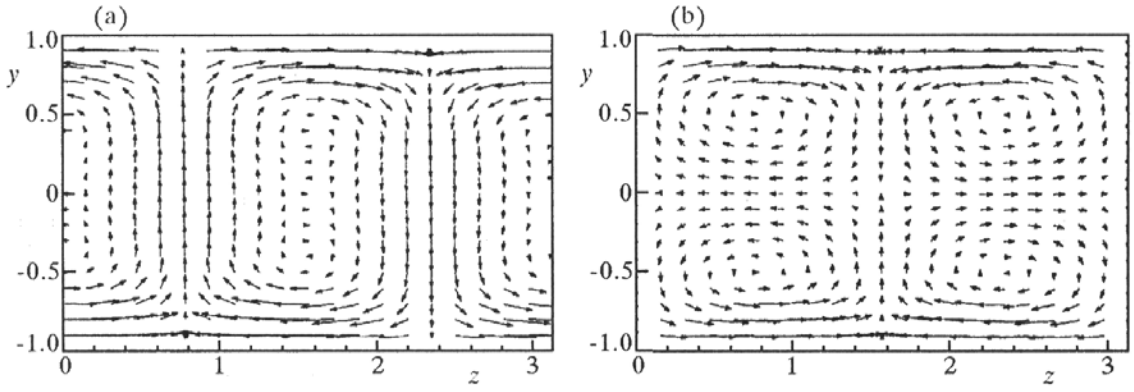

Fig. 2. The spanwise structure of the disturbance velocity fields corresponding to the first (a) and second (b) unstable modes, computed for Re=5000, $\alpha = 3$, $\beta = 2$, $S = 6 \cdot 10^{-3}$ and $\phi = \pi$ (anti-symmetric suction)

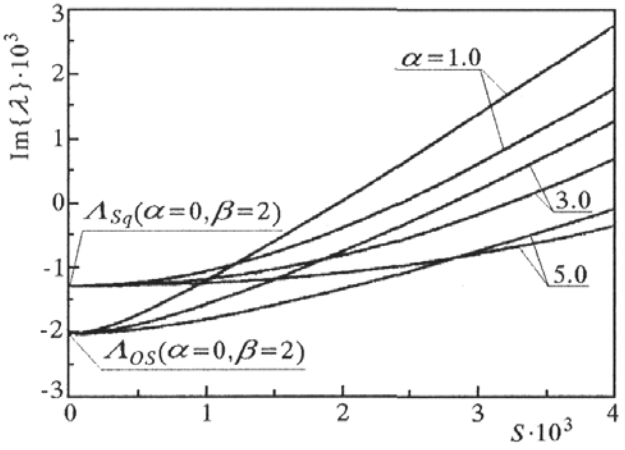

Fig. 3. Amplification rates of the unstable modes plotted versus the suction amplitude S, at various values of the suction wave number α. The other parameters are $\beta = 2$, Re=5000 and $\phi = 0$

Fig. 3. Each line in the plot corresponds to a different value of the suction wave number α, and the value of the spanwise wave number is $\beta = 2$. When the suction amplitudes diminish to zero, the imaginary part of each mode achieves a limit value, which is independent on the suction wave number α and the phase shift ϕ. These numbers can be recognized as the eigenvalues belonging to the spectrum computed for the Poiseuille flow with the wave numbers $\alpha = 0$ and $\beta = 2$. The upper limit actually corresponds to the least damped Squire's mode, while the lower limit is the eigenvalue of the least damped Orr-Sommerfeld's mode (see Appendix for definition of these modes). Since their streamwise wave number is zero, the corresponding eigensolutions do not

depend on the streamwise variable x. The description of essential properties of these modes is provided in the Appendix.

The question arises, which unstable mode originates from Squire's mode and which one from Orr-Sommerfeld's one. It seems to be obvious from Fig. 3 that the first unstable mode is the suction-modulated Orr-Sommerfeld's mode, while the second one seems to be the Squire's mode. This conclusion, however, is not necessarily correct. It is clear from Fig. 3 that, for any fixed value of α, two lines actually intersect before they hit the vertical axis. In other words, there is a value of the suction amplitude when two eigenvalues coincide. The existence of a double eigenvalue may be a generic property of the problem but it might be also an effect of the assumed symmetry of the wall suction. To resolve this issue one has to apply the tracing procedure to a non-symmetric case. In order to brake the symmetry one can change the phase shift between the lower and upper wall distributions of the suction, make the suction amplitudes different, or do both. Actually, the computations show that the phase shift does not change qualitatively the arrangement of lines in Fig. 3. Thus, breaking the symmetry means applying the suction with different amplitudes at the bottom and the upper walls. Figure 4 shows the results. Evidently, in non-symmetric cases the double eigenvalue does not appear – the lines remain separated all way long to the limits at $S_L = S_U = 0$.

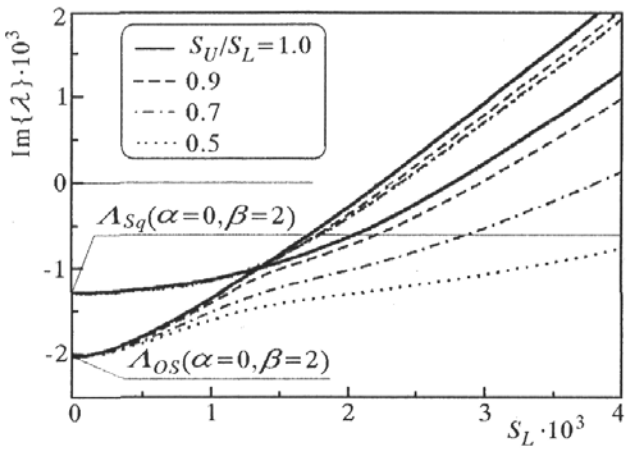

Fig. 4. Amplification rates of the unstable modes plotted as functions of the suction amplitude at the bottom wall S_L. The suction amplitude at the upper wall S_U is equal to a fraction of S_L (non-symmetric suction). The other parameters are fixed and following: Re=5000, $\alpha = 1.8$, $\beta = 2$ and $\phi = 0$

This result shows clearly that the interpretation of the origins of the unstable modes previously suggested by Fig. 3 is actually opposite to the correct one. The first unstable mode should be interpreted as a suction-modulated Squire's

mode, while the second one, as an Orr-Sommerfeld's mode. Closer analysis of the spectrum can establish analogous interpretation for all purely imaginary eigenvalues – all of them are either Squire's or Orr-Sommerfeld's modes, originally streamwise-invariant, "modulated" by the wall suction.

In the remaining part of this section, we discussed some further properties of the unstable modes. We will investigate the influence of the phase shift and other variants of the non-symmetric suction. The results will demonstrate that Squire's and Orr-Sommerfeld's modes respond quite differently to various modes of the suction.

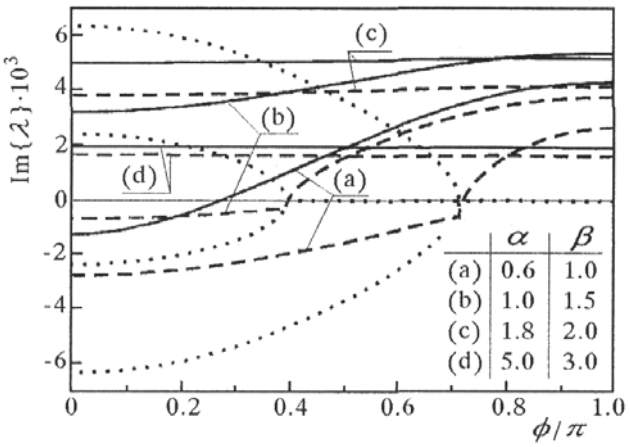

Fig. 5. Amplification rates plotted versus the phase shift ϕ. The solid lines correspond to the Squire mode, while the dashed ones to the Orr-Sommerfeld mode. The dotted lines refer to the real part of the eigenvalue of the OS mode, showing the "splitting" effect (details in text). The suction amplitudes at both wall are equal $S_L = S_U = 6 \cdot 10^{-3}$

The effect of the phase shift on both unstable modes is shown in Fig. 5. These results have been obtained for the suction amplitudes $S_L = S_U = 6.0 \cdot 10^{-3}$. The following observations should be made:

- the anti-symmetric suction ($\phi = \pi$) leads to a more unstable flow than the symmetric one ($\phi = 0$); any other phase shift gives the amplification rate in between,
- the effect of the phase shift becomes negligible for higher values of the suction wave number α,
- when the suction wave is sufficiently long, (or, equivalently, the wave number α is small) there exists a phase shift value where Orr-Sommerfeld's mode splits into a pair of slowly moving wave-like disturbances. This means that the purely imaginary eigenvalue is replaced by

a pair of complex eigenvalues with small, real parts of the opposite sign, and identical imaginary parts. For instance, such splitting for $\alpha = 1$ and $\beta = 1.5$ occurs when $\phi/\pi \approx 0.38$. The reader may notice that the imaginary part (dashed line) of the eigenvalue changes continuously, however the variation is not differentiable. On the left side of the splitting point, the two eigenvalues with opposite real parts (dotted lines) replace the single, purely imaginary eigenvalue existing on the right side.

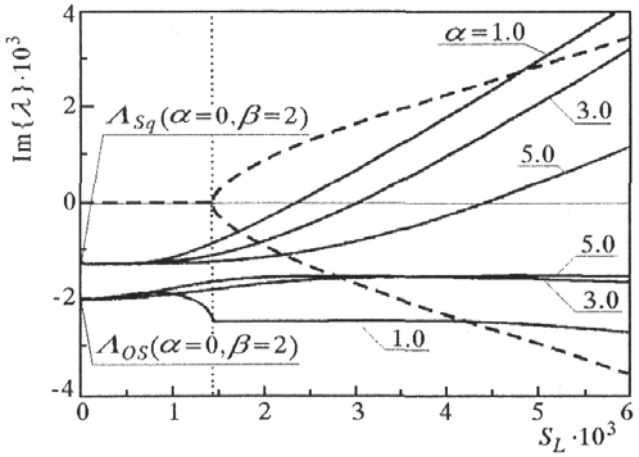

Fig. 6. Amplification rates of the main Squire and Orr-Sommerfeld modes plotted as functions of the suction amplitude at the bottom wall S_L. There is no suction at the upper wall ($S_U = 0$). The other parameters are Re=5000 and $\beta = 2$. The dashed lines refer to the real part of the eigenvalue of the OS mode, demonstrating the "splitting" effect

This splitting (or bifurcation) phenomenon affects only Orr-Sommerfeld's mode, at least in the range of the parameters studied in this work. Similar behaviour characterises Orr-Sommerfeld's mode in the case of non-symmetric or one-sided suction. In the latter case, the suction is applied only at the bottom wall. The results for $\beta = 2$ and three different values of the suction wave number α have been presented in Fig. 6. Again, the variation of the eigenvalue corresponding to Squire's mode is smooth independently of the value of α, while the Orr-Sommerfeld's eigenvalue experiences the split near the value $S_L \approx 1.4 \cdot 10^{-3}$. The real parts of the branching eigenvalues are plotted with a dashed line. Interestingly, the imaginary parts of these eigenvalues depend weakly on the suction amplitude and are negative, i.e. the corresponding travelling disturbances are always stable.

It can be also demonstrated that the branching phenomenon for Orr-Sommerfeld's mode occurs even for symmetric suction providing that the suction wave is sufficiently long. This is shown in Fig. 7 presenting the results

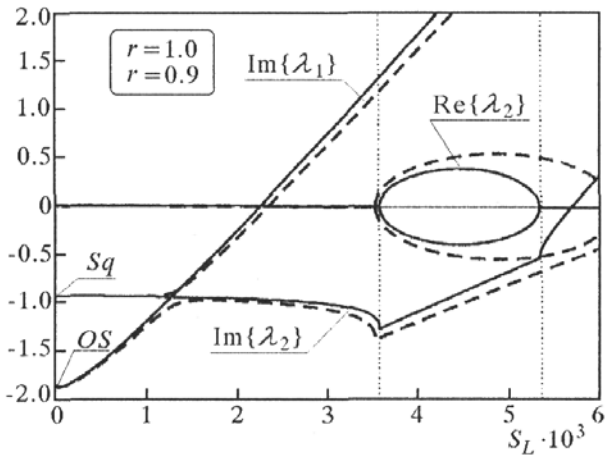

Fig. 7. An example of the "splitting" of the OS eigenvalue occurring in the symmetric (solid lines) and nearly symmetric (dashed line) cases of the wall suction. There exists a closed interval of the suction amplitudes, where the (stable) Orr-Sommerfeld mode is replaced by slowly moving wave-like eigenmodes. The results have been obtained for Re=5000, $\alpha = 1.12$ and $\beta = 1.5$

obtained for $\alpha = 1.12$ and $\beta = 1.5$. The continuous lines correspond to the symmetric case $r = S_U/S_L = 1$, and the dashed lines correspond to the broken symmetry with $r = 0.9$. Again, the removal of the double eigenvalue by braking the symmetry is visible. The Orr-Sommerfeld mode exists in the spectrum from $S_L = 0$ up to $S_L \approx 3.55 \cdot 10^{-3}$. While S_L increases, the Orr-Sommerfeld mode is replaced by a pair of slowly moving wave-like modes. They are still stable and their velocity attains the maximum at $S_L \approx 4.36 \cdot 10^{-3}$. The reader may notice that these waves are indeed very slow – their maximum velocity is of the order 10^{-3}. When the suction amplitude $S_L \approx 5.4 \cdot 10^{-3}$, the eigenvalues coalesce to re-create "ordinary" Orr-Sommerfeld's mode, i.e. the mode, whose eigenvalue has the zero real part. According to the computed results, the splitting and merging phenomena always occur in the stable region.

Consider now the eigenvalue tracing when the suction amplitude at the upper wall is fixed $S_U = 6.0 \cdot 10^{-3}$ and the suction amplitude at the lower wall S_L is gradually reduced from the value of S_U down to zero. The results computed for different combinations of the wave numbers α and β and the phase shift $\phi = 0$ are presented in Fig. 8. It can be noticed that the eigenvalue corresponding to the Squire mode rather weakly responds to the decreasing of the suction amplitude S_L. The amplification rates for the one-sided suction and both-sided symmetric suction are similar. The difference would be more pronounced for the phase shift $\phi = \pi$ (see Fig. 4), but the conclusion is similar: one-sided suction and both-sided suction have nearly the same effect on the

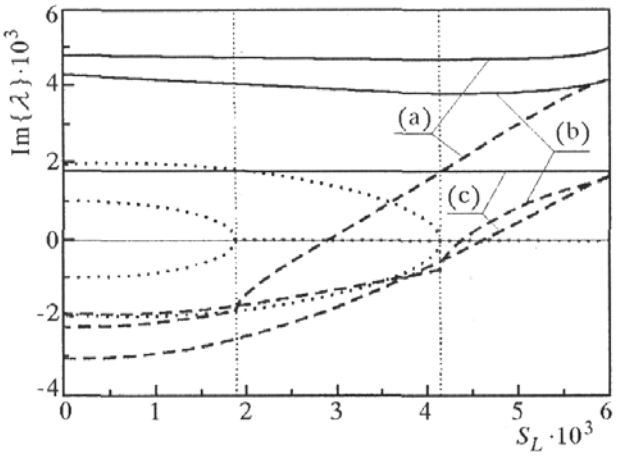

Fig. 8. Amplification rates of the Squire (solid line) and Orr-Sommerfeld (dashed line) modes plotted versus the suction amplitude at the bottom wall S_L. The magnitude of the suction at the upper wall is fixed and equal $S_U = 6 \cdot 10^{-3}$. The results have been obtained for Re=5000, $\phi = 0$ and following wave numbers: (a) $\alpha = 1.2$, $\beta = 1.5$, (b) $\alpha = 2.0$, $\beta = 2.5$, (c) $\alpha = 5.0$, $\beta = 3.5$

overall flow stability. In contrast to Squire's mode, the Orr-Sommerfeld's one is highly sensitive to the ratio S_L/S_U. When the bottom suction is sufficiently small the Orr-Sommerfeld mode becomes stable and the only unstable disturbance form is the Squire mode. With further decrease of the amplitude S_L the splitting is observed and the Orr-Sommerfeld mode disappears from the spectrum.

5. Concluding remarks

The presence of the wall suction essentially changes stability properties of a viscous flow in a channel. Originally stable disturbance modes respond to space-periodic modulation of the main flow, become streamwise dependent and loose their stability at much lower Reynolds number than TS waves in the original Poiseuille flow.

Two unstable modes of different origin can coexist within a wide parameter range. Although their geometrical structures are similar, the Orr-Sommerfeld and Squire modes behave very differently in the presence of non-symmetric suction distributions.

It is worth reminding that the modes with zero streamwise wave number appear in the problem of determination of transient growth of the disturbances

in the Poiseuille flow (see for instance Butler and Farrel (1992) or Reddy and Henningson (1993)). If the Reynolds number is less than critical, all sufficiently small disturbances injected into the flow eventually decay in time. However, due to the non-normality of the underlying differential operator, some forms of the disturbances can temporarily grow in time achieving magnitudes (in the sense of the kinetic energy) several orders higher that the initial ones. Recent studies on the onset of turbulence in shear flows emphasize a crucial role of this sub-critical energy growth in the initial stages of the transition process. The most recent survey on this theory can be found in the monograph Schmidt and Henningson (2001).

Appendix – Special Orr-Sommerfeld and Squire modes

We summarize here the basics of the linear stability theory for parallel flows (see for instance Schmidt and Henningson, 2001). Consider a flow between two parallel planes. The direction of y-coordinate of the Cartesian reference frame is assumed perpendicular to the boundaries of the flow domain, and the range of the latter in the y direction is $[-1,1]$. The velocity field of the basic flow is defined as follows

$$\boldsymbol{V}_0 = [u_0(y), 0, w_0(y)] \tag{A.1}$$

The disturbance velocity and pressure fields can be assumed in the from of the Fourier modes

$$\begin{aligned} \boldsymbol{v} &= [g_u(y), g_v(y), g_w(y)] \exp[\mathrm{i}(\alpha x + \beta z - \sigma t)] \\ p &= q(y) \exp[\mathrm{i}(\alpha x + \beta z - \sigma t)] \end{aligned} \tag{A.2}$$

The stability equations can be derived in terms of primitive variables. They will contain the amplitude functions of the Cartesian components of the velocity field $\boldsymbol{v}$ and the pressure p. It is, however, possible to obtain the stability equations in the form involving only two unknowns: the function g_v and the amplitude function for the y-component of the disturbance vorticity field denoted as η. Using the definition of the vorticity, one has

$$\eta = \mathrm{i}(\beta g_u - \alpha g_w) \tag{A.3}$$

The continuity equation applied to the disturbance velocity field yields another relation

$$\alpha g_u + \beta g_w = \mathrm{i} D g_v \tag{A.4}$$

where $D \equiv d/dy$.

Hence, the knowledge of the wall-normal components of the velocity and vorticity fields is sufficient to determine the remaining components of the velocity field. Namely, from (A.3) and (A.4) we have

$$g_u = \frac{1}{k^2}\mathrm{i}(\alpha D g_v - \beta\eta) \qquad g_w = \frac{1}{k^2}\mathrm{i}(\beta D g_v + \alpha\eta) \tag{A.5}$$

In the above the symbol k denotes the length of the disturbance wave vector, i.e. $k = \sqrt{\alpha^2 + \beta^2}$.

The stability equation can be written as follows

$$\begin{gathered}\Big\{(D^2 - k^2)^2 - \mathrm{iRe}[(\alpha u_0 + \beta w_0 - \sigma)(D^2 - k^2) - D^2(\alpha u_0 + \beta w_0)]\Big\} g_v = 0 \\ [D^2 - k^2 - \mathrm{iRe}(\alpha u_0 + \beta w_0 - \sigma)]\eta - \mathrm{iRe} D(\beta u_0 - \alpha w_0) g_v = 0\end{gathered} \tag{A.6}$$

The amplitude functions in (A.6) should satisfy the following homogeneous boundary conditions

$$g_v(\pm 1) = 0 \qquad D g_v(\pm 1) = 0 \qquad \eta(\pm 1) = 0 \tag{A.7}$$

Equations (A.6) accompanied by boundary conditions (A.7) state a differential eigenvalue problem. There are two classes of nontrivial solutions. If the wave number σ is an eigenvalue of fourth-order differential boundary problem $(\mathrm{A.6})_1$ and $(\mathrm{A.7})_{1,2}$ then a nontrivial solution g_v to this problem exists. Second-order boundary problem $(\mathrm{A.6})_2$ and $(\mathrm{A.7})_3$ is then uniquely (modulo normalization of g_v) solvable for the amplitude function η (providing that σ is not an eigenvalue of the corresponding differential operator). The remaining components of the corresponding velocity field can be evaluated from (A.5). The complete eigensolutions of this kind are called Orr-Sommerfeld's modes.

The other class of solutions is called the Squire modes. If the wave number σ does not belong to the spectrum of $(\mathrm{A.6})_1$, $(\mathrm{A.7})_{1,2}$, then the only solution to this problem is trivial $g_v \equiv 0$. Then, second-order differential problem $(\mathrm{A.6})_2$ and $(\mathrm{A.7})_3$ becomes uncoupled and has a nontrivial solution when σ belongs to the spectrum of the corresponding second-order differential operator, i.e. to the Squire spectrum. In contrast to Orr-Sommerfeld's modes, Squire's ones describe purely horizontal motion of the fluid defined by the following amplitude functions

$$g_u = -\frac{1}{k^2}\mathrm{i}\beta\eta \qquad g_w = \frac{1}{k^2}\mathrm{i}\alpha\eta \tag{A.8}$$

In the remaining part of Appendix, we will focus on the special case arising in the context of the current study. Namely, we will consider the case of the standard Poiseuille flow. Thus, we have $u_0 = 1 - y^2$ and $w_0 = 0$. Next, we

will consider the disturbance modes with the streamwise wave number $\alpha = 0$. Such modes are dependent solely on two spatial variables y and z. We start the analysis with the Squire modes. They are defined as eigensolutions to the following problem

$$(D^2 - \beta^2 + \mathrm{iRe}\sigma)\eta = 0 \qquad \eta(\pm 1) = 0 \tag{A.9}$$

One should note an important feature of problem (A.9) – the velocity of the reference flow does not appear in the coefficients of the differential operator.

Assume that $\sigma = \mathrm{i}\sigma_i$ for a certain $\sigma_i \in R$. One obtains the following differential eigenvalue problem with constant coefficients

$$D^2\eta - (\beta^2 + \sigma_i \mathrm{Re})\eta = 0 \qquad \eta(\pm 1) = 0 \tag{A.10}$$

Nontrivial solutions exist only when the following equality

$$-(\beta^2 + \sigma_i \mathrm{Re}) = \frac{m^2\pi^2}{4}$$

holds for any integer m, which yields the following eigenvalues

$$\sigma_i(m) = -\frac{4\beta^2 + m^2\pi^2}{4\mathrm{Re}} \tag{A.11}$$

The corresponding eigenfunctions are

$$\varphi_m(y) = \begin{cases} \cos\dfrac{\pi m}{2} & \text{for} \quad m-\text{odd} \\ \sin\dfrac{\pi m}{2} & \text{for} \quad m-\text{even} \end{cases} \tag{A.12}$$

It can be shown that formula (A.11) describes all eigenvalues of boundary problem (A.9). This means that all eigenvalues of (A.9) are purely imaginary numbers and, since all $\sigma_i(m)$ are negative, all Squire's modes with $\alpha = 0$ are stable.

Consider now boundary problem $(\mathrm{A.6})_1$, $(\mathrm{A.7})_{1,2}$ with the same assumptions as in the above. This time we have the following fourth-order eigenvalue problem

$$\begin{aligned} &(D^2 - \beta^2)(D^2 - \beta^2 + \mathrm{iRe}\sigma)g_v = 0 \\ &g_v(\pm 1) = Dg_v(\pm 1) = 0 \end{aligned} \tag{A.13}$$

Again, the velocity field of the reference flow has disappeared from the equation, and we deal with a differential problem with constant coefficients. Inserting the particular solution $g_v(y) = \exp(\lambda y)$ and assuming that $\sigma = \mathrm{i}\sigma_i$ we get four characteristic exponents

$$\lambda_{1,2} = \pm\beta \qquad \lambda_{3,4} = \pm\sqrt{\beta^2 + \sigma_i \mathrm{Re}}$$

Thus, the general solution has the following form

$$\begin{aligned} g_v(y) &= C_1 \cosh(\beta y) + C_2 \sinh(\beta y) + \\ &+ C_3 \cos\sqrt{-(\beta^2 + \sigma_i \mathrm{Re})} + C_4 \sin\sqrt{-(\beta^2 + \sigma_i \mathrm{Re})} \end{aligned} \tag{A.14}$$

In (A.14), the inequality $\beta^2 + \sigma_i \mathrm{Re} < 0$ has been assumed.

The homogeneous boundary conditions lead to a system of four linear equations for the coefficients $C_1, ..., C_4$. The symmetry properties of the trigonometric and hyperbolic functions in the range $[-1, 1]$ allow for splitting this system into two separate subsystems for the symmetric and anti-symmetric eigensolutions, namely

$$\begin{bmatrix} \cosh\beta & \cosh\sqrt{\beta^2 + \sigma_i \mathrm{Re}} \\ \beta\sinh\beta & \sqrt{\beta^2 + \sigma_i \mathrm{Re}}\sinh\sqrt{\beta^2 + \sigma_i \mathrm{Re}} \end{bmatrix} \begin{bmatrix} C_1 \\ C_3 \end{bmatrix} = \mathbf{0}$$

$$\begin{bmatrix} \sinh\beta & \sinh\sqrt{\beta^2 + \sigma_i \mathrm{Re}} \\ \beta\cosh\beta & \sqrt{\beta^2 + \sigma_i \mathrm{Re}}\cosh\sqrt{\beta^2 + \sigma_i \mathrm{Re}} \end{bmatrix} \begin{bmatrix} C_2 \\ C_4 \end{bmatrix} = \mathbf{0} \tag{A.15}$$

Consider equation $(\mathrm{A.15})_1$. Assuming that $\beta^2 + \sigma_i \mathrm{Re} < 0$, nontrivial solutions exist only when the following equality holds

$$\sqrt{-(\beta^2 + \sigma_i \mathrm{Re})}\,\tan\left(\sqrt{-(\beta^2 + \sigma_i \mathrm{Re})}\right) + \beta\tanh\beta = 0 \tag{A.16}$$

The above equation has the form

$$x\tan x + H = 0 \qquad H > 0 \tag{A.17}$$

and it has infinitely many solutions in $[0, +\infty)$. These solutions determine the eigenvalues as follows

$$\sigma_i(m) = -\frac{\beta^2 + x_*(m)}{\mathrm{Re}} \qquad m = 1, 2, ... \tag{A.18}$$

The smallest solution $x_*(1)$ is located inside $(\pi/2, \pi)$. It corresponds to the least damped symmetric eigensolution.

System $(A.15)_2$ has a nontrivial solution only when the following equality holds (again, we assume that $\beta^2 + \sigma_i \mathrm{Re} < 0$

$$\sqrt{-(\beta^2 + \sigma_i \mathrm{Re})}\, \cot\left(\sqrt{-(\beta^2 + \sigma_i \mathrm{Re})}\right) - \beta \coth \beta = 0 \tag{A.19}$$

The above equation has the following form

$$x \cot x + H = 0 \qquad H < 0 \tag{A.20}$$

It is easy to show that actually $H \leqslant -1$. Therefore, the smallest solution $x_*(1)$ is located inside the interval $(\pi, 3\pi/2)$. Hence, the least damped antisymmetric eigensolution has stronger damping than the least damped symmetric eigensolution.

It can be shown that if $\beta^2 + \sigma_i \mathrm{Re} \geqslant 0$ the problem has only a trivial solution. Thus, boundary problem (A.13) does not have any other eigenvalues. Additionally, all eigenvalues are purely imaginary and, since all $\sigma_i(m)$ are negative, all Orr-Sommerfeld's modes with $\alpha = 0$ are stable.

We will prove that the imaginary part of each eigenvalue of boundary problem (A.13) attains a local maximum at a certain value of the spanwise wave number $\beta \neq 0$. It is equivalent to show that the function $S(\beta) = \beta^2 + x_*^2$ has a local minimum. Here, x_* denotes one of the solutions to the algebraic equation

$$x \tan x + \beta \tanh \beta = 0 \tag{A.21}$$

At the extremum, the derivative of $S(\beta)$ must vanish

$$S'_m(\beta_e) = 2\beta_e + 2x_{*,m} x'_{*,m} = 0 \tag{A.22}$$

The derivative $x'_{*,m}$ can be expressed with the use of the Implicit Function Theorem applied to the function $F(x, \beta) = x \tan x + \beta \tanh \beta$. Hence

$$x'_{*,m} = -\frac{\partial F/\partial \beta}{\partial F/\partial x} = -\frac{\tanh \beta + \beta(1 - \tanh^2 \beta)}{\tan x + x(1 + \tan^2 x)} \tag{A.23}$$

In the above x_e denotes the solution to (A.21) corresponding to $\beta = \beta_e$. This way one has a pair of equations for the unknowns (β_e, x_e)

$$\begin{aligned} &\beta_e - x_e \frac{\tanh \beta_e + \beta_e(1 - \tanh^2 \beta_e)}{\tan x_e + x_e(1 + \tan^2 x_e)} = 0 \\ &x_e \tan x_e + \beta_e \tanh \beta_e = 0 \end{aligned} \tag{A.24}$$

After some algebra, the following relation can be derived from (A.24)

$$(x_e^2 + \beta_e^2)(1 - \beta_e \tanh \beta_e) \tanh \beta_e = 0 \tag{A.25}$$

Equation (A.25) holds if:

1) $x_e = \beta_e = 0$ – this leads to the zero value of σ_i, which is excluded (zero is not an eigenvalue of the problem),

2) $\beta_e = 0$ – yields "trivial" solution: the derivative $S'_m(0) = 0$ because of the symmetry with respect to the spanwise wave number β,

3) β_e is a solution to the algebraic equation $\beta_e \tanh \beta_e = 1$.

In the last case, the solution is $\beta_e = 1.199678640...$.

We will show that the function $S(\beta)$ attains its local minimum $\beta = \beta_e$. We need to compute the second derivative

$$S''(\beta) = 2 + 2[x'_{*,m}(\beta)]^2 + 2x_{*,m}(\beta)x''_{*,m}(\beta) \tag{A.26}$$

at $\beta = \beta_e$. By differentiating formulae (A.23), it can be shown that $x''_{*,m}(\beta_e) = 0$. Thus

$$S(\beta_e) = 2 + 2[x'_{*,m}(\beta_e)]^2 > 0 \tag{A.27}$$

i.e. $S(\beta_e)$ is a local minimum. The corresponding eigenvalue $\sigma_{e,m} = -S(\beta_e)/\mathrm{Re}$ attains the local maximum. For example, we have $\sigma_{e,1} = -0.0018540387...$ for Re=5000.

Similar argumentation can be given for the anti-symmetric Orr-Sommerfeld modes.

References

1. BUTLER K.M., FARREL B.F., 1992, Three-dimensional optimal perturbations in viscous shear flow, *Physics of Fluids A*, **4**, 8

2. CABAL T., SZUMBARSKI J., FLORYAN J.M., 2002, Stability of flow in a wavy channel, *Journal of Fluid Mechanics*, **457**, 191-212

3. FLORYAN J.M., 1997, Stability of wall-bounded shear layers in the presence of simulated distributed surface roughness, *Journal of Fluid Mechanics*, **335**, 29-55

4. REDDY S.C., HENNINGSON D.S., 1993, Energy growth in viscous channel flows, *Journal of Fluid Mechanics*, **252**, 209-238

5. SAAD Y., 1992, *Numerical Methods for Large Eigenvalue Problems*, Halstead Press, New York

6. SCHMIDT P.J., HENNINGSON D.S., 2001, Stability and transition in shear flows, *AMS*, **142**, Springer-Verlag New York

7. SZUMBARSKI J., FLORYAN J.M., 1999, A direct spectral method for determination of flows over corrugated boundaries, *Journal of Computational Physics*, **153**, 378-402

O pochodzeniu niestatecznych form zaburzeń w przepływie cieczy lepkiej w kanale z przestrzennie okresowym odsysaniem/wypływem

Streszczenie

W pracy rozważa się zagadnienie liniowej stateczności przepływu cieczy w płaskim kanale, w obecności periodycznie rozłożonego odsysania/wypływu przez ściany. Celem analizy jest identyfikacja zaburzeń krytycznych i objaśnienia ich związku z rozwiązaniami własnymi zagadnienia stateczności dla przepływu Poiseuille'a. Stosując metodę kontynuacji wartości i rozwiązań własnych po parametrze wykazano, że obserwowane formy niestabilności to zmodyfikowane okresowo w kierunku przepływu poprzeczne, symetryczne mody Squire'a i Orra-Sommerfelda, którym odpowiadają czysto urojone wartości własne. Zbadano numerycznie wpływ parametrów odsysania/wypływu na własności tych modów.

Manuscript received January 17, 2002; accepted for print March 22, 2002